האוניברסיטה העברית בירושלים
THE HEBREW UNIVERSITY OF JERUSALEM

עבודת גמר לתואר מוסמך במדעי הטבע בנושא:

הדפסת אלמנטים אופטיים תלת מימדיים ישירות על קצה סיב אופטי

Direct 3D Nano-Printing of optical elements on Optical Fiber Tip

By

Israel Weiss

This work was done under the supervision of

Prof. Dan Marom

A thesis submitted in partial fulfillment for the

requirements for the degree of

Master of Science

Faculty of Science

Department of Applied Physics

אדר ה'תשע"ו

March 2016

Acknowledgements

I would like to thank my advisor Prof. Dan Marom for his guidance and advices through the research. For his availability every time questions aroused.

Many thanks to all the members of the Photonic Devices group for their reviews, ideas and suggestions.

I wish to thank Brojde Center for their support, advice and use of the nanoscribe system, especially Ms. Yehudit Garcia.

I wish to thank my family, who supported me all along the way.

Special thanks to my wife, Revital, for her endless support and encouragement through the research. Without her, this work couldn't succeed.

Finally, I wish to thank God in heaven "for it is he who gives you the ability to produce wealth".

Abstract

In this work I report on the development and optimization of fabrication process of three dimensional optical nano devices directly on the tip of optical fiber.

The system we use in order to realize these optical elements is the commercial Nanoscribe™ system which is based on polymerization of negative tone photoresist, and using two-photon absorption.

Many efforts were invested in this research in two main directions. One is the optimization of the element's optical quality, by reducing its surface's roughness and second is the system's adaptation to print elements directly on an optical fiber tip, in accurate form and exact alignment to the optical axis of the fiber.

We utilize the ability to print arbitrary real 3D volumetric structures in photoresist at the nanoscale with our Nanoscribe tool directly onto a fiber tip in convenient and accurate way, and this ability gives us wide leeway for realizing sophisticated optical elements that are directly interact with the beam delivered by the fiber.

תקציר

בעבודה זו אני מדווח על פיתוח ואופטימיזציה של תהליך יצור של רכיבים אופטיים ננומטרים תלת מימדיים המודפסים ישירות על קצה סיב אופטי.

המערכת בה השתמשנו לצורך המחקר היא מערכת של חברת ™Nanoscribe, המדפיסה אלמנטים בעזרת פילמור פוטורזיסט שלילי, ומבוססת על תהליך לא לינארי של בליעת שני פוטונים (Two Photon Absorption).

מאמצים רבים הושקעו במחקר זה בשני תחומים מרכזיים. אחד הוא אופטימיזציה של האיכות האופטית של האלמנט המפולמר, מבחינת הצורה הסופית של האלמנט המיוצר, ובהורדת חיספוס פני השטח ויצירת מבנים חלקים. התחום השני הוא התאמת המערכת ליצירת מבנים על קצה סיב אופטי, באופן מדויק ומיושר לציר האופטי של הסיב.

יכולת זו ליצור אלמנטים אופטיים ישירות על קצה הסיב מאפשרת לממש מגוון רחב של תחומים ואלמנטים מורכבים ומסובכים, שבאים באינטרקציה עם האור היוצא מהסיב.

Table of Contents

1 Introduction and Motivation

Optical fibers, which are widely used all over the world, allows efficient transport of light to extended ranges and across harsh environments. They carry the vast majority of optical communication information to end users, and increasingly being used for sensing applications. One of the favorable attributes of an optical fiber is that the guided light in the fiber’s core is well protected from the environment by the cladding and additional encapsulating polymers. However naturally, in data extraction and processing as well as in many sensing applications, the light is needed to exit the fiber and interact with the surrounding environment.

The traditional way to control and manipulate the light is using free space optics elements. However, there is an option to realize micro-optics devices directly on the fiber tip, for getting more efficiency and accuracy. Such fiber tip devices enable diverse applications that benefit from the fiber delivery, as well as the well-defined air interface, such as remote optical sensing, biomedicine, beam shaping, opto-mechanical systems etc.

In order to realize such optical devices, we use a three-dimensional (3D) printing tool to create modifying element directly at the fiber tip and integrated with it. The system we used is the commercial Nanoscribe™ system which is implemented by polymerization of negative photoresist, formed when a writing optical Gaussian beam is tightly focused and its intensity squared value exceeds the polymerization threshold (based on two-photon excitation). We utilize the ability to print arbitrary real 3D volumetric structures at the nanoscale with our Nanoscribe tool directly onto a fiber tip in convenient and accurate way, and this ability gives us wide leeway for realizing sophisticated optical elements that directly interact with the beam delivered in the fiber.

2 Scientific and Technical Background

2.1 Common solutions

Realization of optical elements on an optical fiber tip has been carried out for several years. For that goal, two main approaches are in use. One is to realize a standalone optical microsystem on a separate substrate, and then transferring and locating it on the fiber tip with some mechanical tools and methods [1]. This method includes difficulties in transferring the device, and has limitations on the size and shape of the device because the need to take it physically and transfer it to another place.

Another method is the direct writing and/or deposition onto the end fiber facet using various lithography techniques. These techniques are typically restricted to planar patterns and surface structures and it is not possible to realize real 3D structures using this method (see figure 1 for examples).

One example is using deposition techniques in order to create patterns on the fiber tip [2]. These techniques sacrifice the arbitrary geometrical control offered by more precise lithographic techniques, but they have the benefit of low overhead cost, providing ready access to the nano-regime.

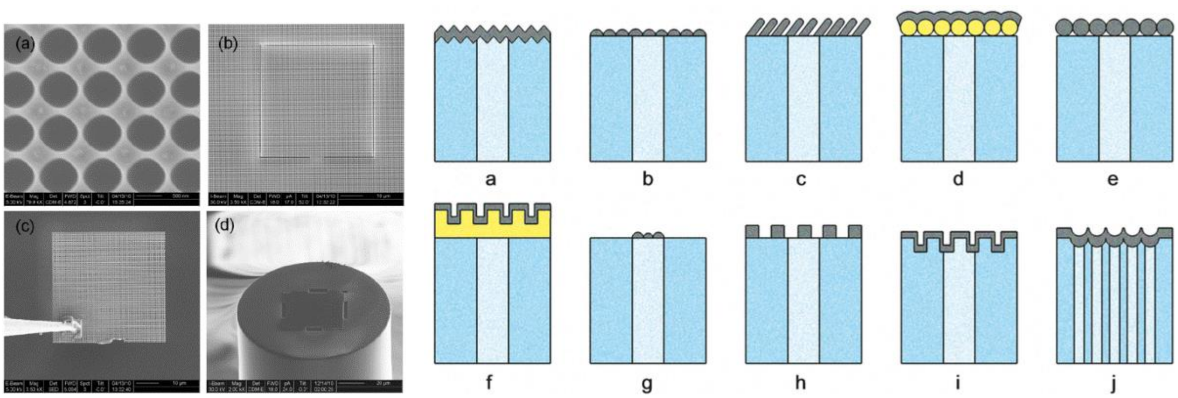

Figure 1: Fiber sensors with direct fiber to free-space interrogation. Left: Microsystem approach where (a) silicon photonic crystal is (b) ion milled, (c) lift and transferred by probe, and (d) bonded onto fiber tip [1]. Right: Schemes for producing surface-enhanced Raman scattering (SERS) probes by nanostructuring of the fiber tip [2].

An additional example is using Focused Ion Beam (FIB) and directly milling the fiber facet in the desired shape, getting a phase plate on top of it (figure 2) [3-4]. Using this method it is possible to realize forms like lenses, phase plates and also asymmetrical structures, but the main disadvantage of this method is the limitation to bulk structures (called 2.5D), by milling it only from top to bottom.

Our research goal is to print optical elements by direct laser lithography on the fiber tip. The main advantage of this method is the possibility to create arbitrary real 3D elements in the nanoscale, including suspended devices and combination of few separate optical elements into complete micro system.

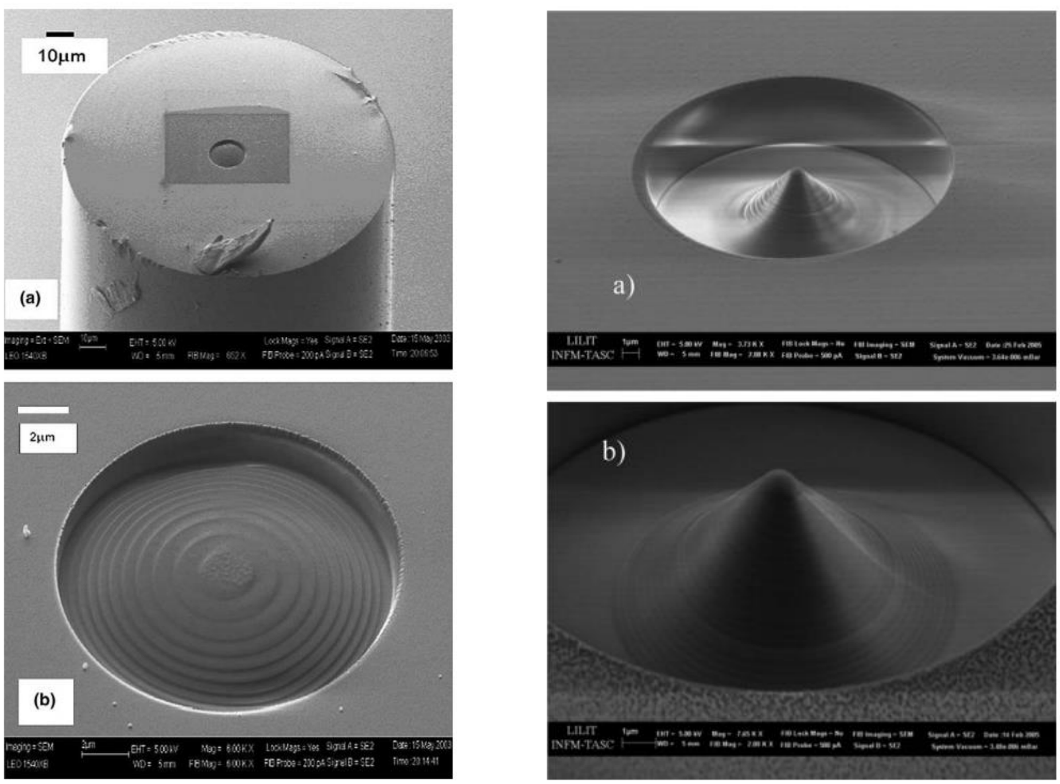

Figure 2: SEM images of FIB milled DOE-microlens (left) and an axicon (right) on top of optical fiber [3-4].

2.2 The “nanoscribe system”

In order to fabricate our devices we use the nanoscribe system which is an advanced commercial 3D printing system, making the process more reliable and convenient and enable us to create arbitrary and complicated structures.

The printing process with the Nanoscribe system is polymerization of a negative photoresist, which is carried out by focusing a laser beam into the volume of the un-polymerized resist in a liquid phase. The process is based on two photon polymerization phenomena (which will be detailed later).

The system uses pulsed femtosecond fiber laser source with center wavelength of 780 nm, repetition rate of about 80 MHz and pulse width of about 100 fs. The laser beam is focused through a high NA immersion objective into the photoresist (which is transparent to the laser wavelength), creating very small volume element with high intensity, enough to initiate the polymerization with two photon absorption effect.

The writing process is performed line after line, by moving the sample using a piezo stage with nm resolution in the operation volume of 300μm×300μm×300μm and by controlling the laser output power for polymerization of the designed structure. The laser spot is fixed in a specific location during the printing process (figure 3).

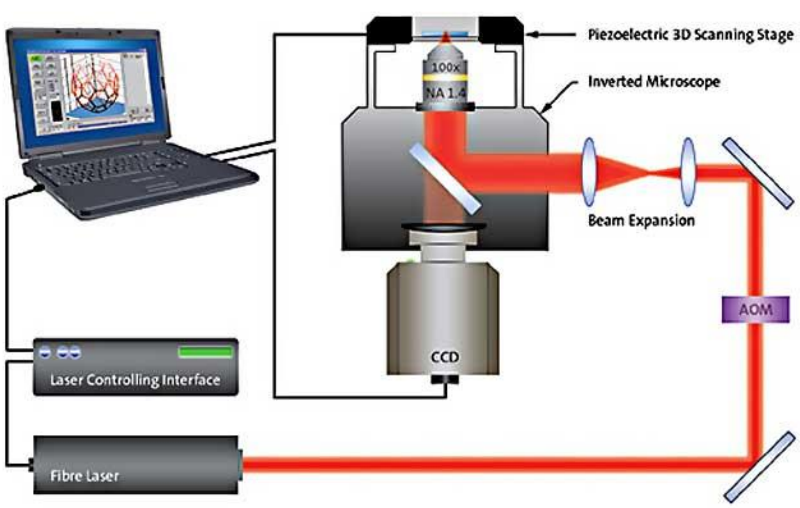

Figure 3: The nanoscribe system operation principle

We use the “IP-Dip” photoresist which is special Nanoscribe designed index-matched photoresist that serves as immersion and photosensitive material simultaneously (will be detailed later). This photoresist offers very high resolution and has no need for preparation before writing (unlike SU-8 resist which requires pre-baking), making the writing process much simpler and immediate.

2.2.1 Two Photon Absorption process

Two Photon Absorption (TPA) is a nonlinear process in which two photons of identical or different frequencies are absorbed by one molecule or atom simultaneously, and excite an electron to higher energy state. The energy difference between the ground and the excited states is the sum of energies of the two photons (figure 4). That process requires very high intensity of light in order to excite the material’s energy state, due to the low probability that two photons will hit one molecule at the same time.

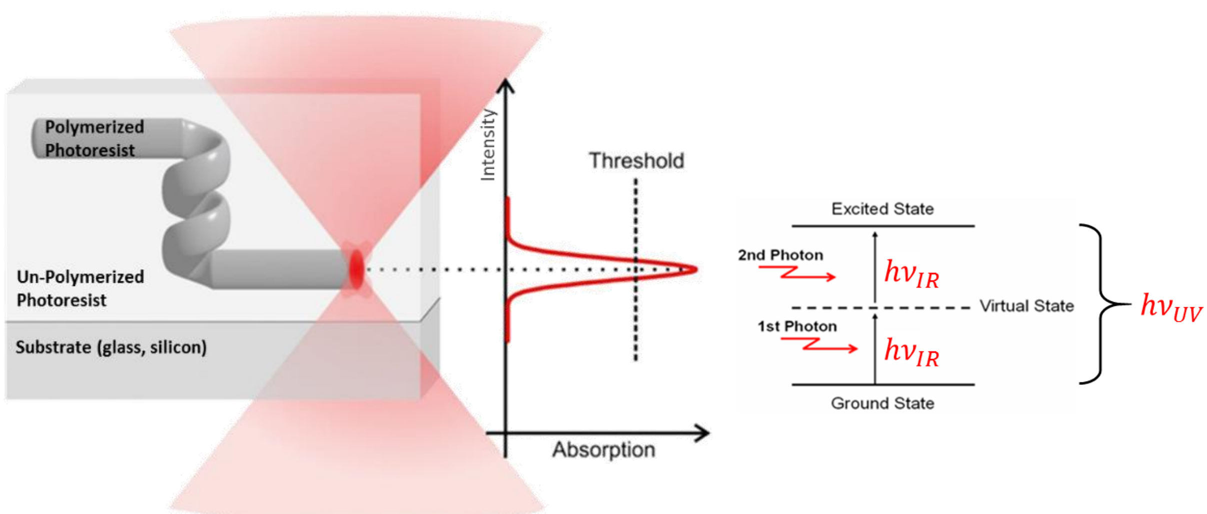

Figure 4: Two photon absorption laser lithography - Principle of oparation (left) and energy states (right)

The expression of the electric field of gaussian beam, assuming linear polarized light in the x axis is:

$$E(r,z) = E_0\hat{x}\frac{\omega_0}{\omega(z)}\exp\left(-\frac{r^2}{\omega(z)^2}\right)\exp\left(-i\left(kz + k\frac{r^2}{2R(z)} - \psi(z)\right)\right) \quad , \quad k = \frac{2\pi}{\lambda}\cdot n$$

Where k is the complex wave number and n is the complex refractive index where:

$$n = n_0 + n_2 I - i\frac{\lambda}{4\pi}(\alpha_0 + \beta_{TPA} I)$$

$$n_2 = \frac{1}{c\cdot n_0^2\cdot \varepsilon_0}\cdot\frac{3}{4}Re\{\chi^{(3)}\} \ , \ \beta_{TPA} = \frac{-\omega}{c^2\cdot n_0^2\cdot\varepsilon_0}\cdot\frac{3}{2}Im\{\chi^{(3)}\}$$

and β_{TPA} is the TPA coefficient. The effect's strength is related to the imaginary part of the third order nonlinear susceptibility $\chi^{(3)}$ which is a property of the material.

In the nanoscribe system, the usage of polymerization with TPA is very important because in that way, only a tightly focused small volume of the laser beam polymerize the resist. The whole region that surrounds the focus of the beam has no effect on the resist because it is actually transparent to the laser wavelength and there is not enough intensity for generating the TPA process (figure 4).

2.2.2 Confocal optics

In confocal systems, which are typically used in confocal microscopy, the laser beam is directed to the specimen using a dichroic mirror (that reflects the light of a specific wavelength range and pass the light of other wavelengths). The beam is focused onto the specimen by high NA objective lens of the microscope. The light emitted from the specimen by fluorescence in response to the laser beam illumination, goes back the same pathway as the laser beam and,

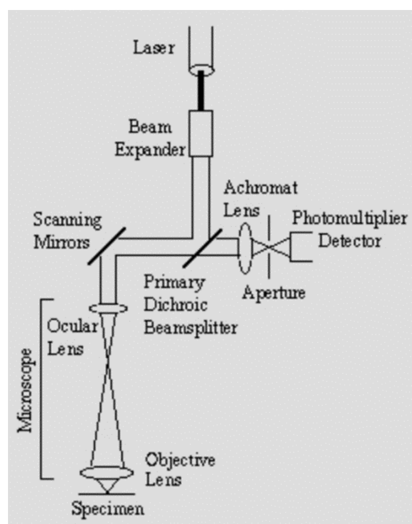

Figure 5: Confocal system principle

this time, passes through the dichroic mirror and focused onto a plane on which only the parallel light beam is focused. The focused beam is selectively passed through an aperture and then detected by a photomultiplier behind the aperture plate (figure 5). In that way the light from the focal point in the specimen is re-focused on the confocal point so that only the light from a specific focal plane is detected.

The nano scale resolution in the system is achieved by using the principle of confocal system. The laser output, i.e. the fiber laser tip of the system, acts as a point source, followed by optics for beam expansion and an objective with very high NA to get a tightly focused laser beam (figures 3-5). The voxel (volume element) with the high power concentration has a prolate spheroid shape with width of ~100-200nm and height of about 1µm (the size of the polymerized volume can be controlled with writing parameters as the laser power and writing velocity).

3 Fabrication and Characterization Methods

3.1 Technical adaptation and alignment

The standard configuration of printing uses high NA oil immersion objective lens, with index-matched oil, allowing an ideal focusing in a resist cast on top of the glass substrate (figure 6 left). The substrate in that configuration needs to be thin and transparent, allowing the laser beam passing through the substrate and print the structure on the other side of it.

That method has limitation on the height of the printed structures because of the working distance of the objective lens, and using that technique, it is impossible to print on big opaque substrates like optical fiber.

In order to print structures on the fiber tip, we used the immersion mode of printing, called Dip-in laser lithography (DiLL) which is a novel concept developed by nanoscribe. In the DiLL process, the objective lens is directly dipped into a liquid photoresist which serves as immersion medium and photosensitive material at the same time and the structure is printed on the closer side of the substrate (figure 6 right).

For DiLL, the height of the structure is not limited by the working distance of the objective lens any more, i.e., high-NA objective lenses with short working distances can

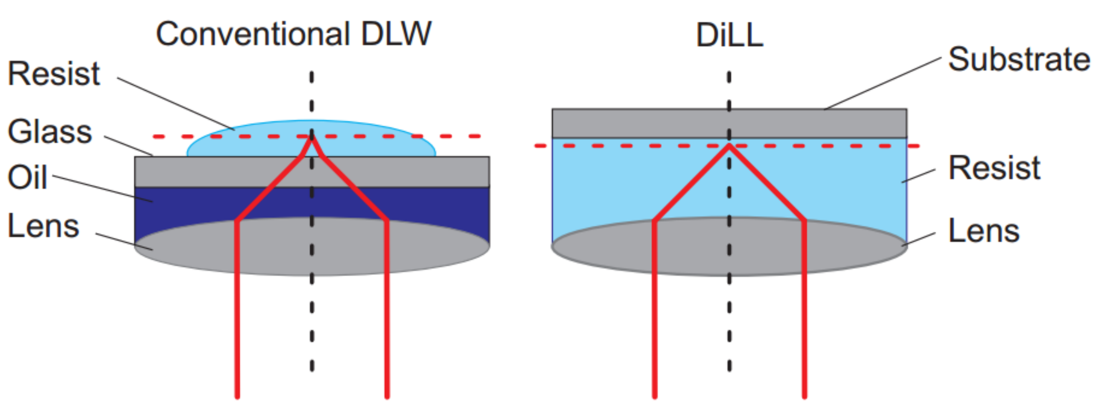

Figure 6: Comparison between the conventional writing configuration (left) and Dip-in Laser Lithography (right)

be used. Accordingly, the best resolution is achieved independent of the writing depth or substrate, and in this scheme, no depth-dependent aberrations occur.

In addition, we have modified the working mechanism of the Nanoscribe substrate, and installed a solution which supports an FC/PC fiber connector and having the fiber end face directly face the microscope objective.

Using this technique we have verified that the system can properly identify the fiber end face (important for properly starting the writing process from the substrate, at z=0, to ensure good adhesion) and recognize the fiber core by sending white light from the other fiber end for x, y grid registration with respect to core (figure 7).

The microscope view in the software has a blue cursor on the screen, for comfort adjustment of the substrate under the laser spot. First, the cursor is located exactly on the laser spot by weak activation of the laser. Then the fiber is moved to be aligned with the cursor for printing the structure in the exact position.

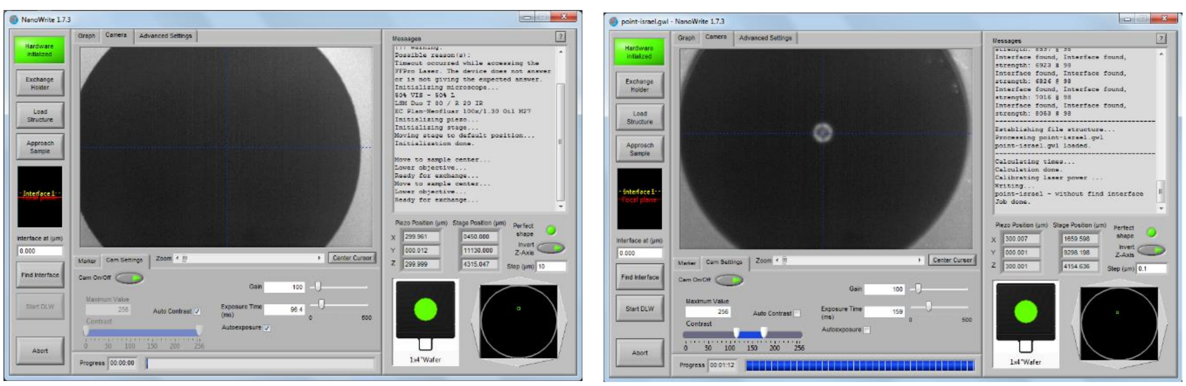

Figure 7: Microscope is focused on the fiber facet in the Nanoscribe software screenshot, before (left) and after (right) alignment to the lightened core.

Additionally we installed a tip-tilt mount for setting the angles on the holder (figure 8). By finding the interface's height at several points around the fiber core, we calculate the angles deviation at x and y axes, and with few iterations we fixed the tilts manually, making the fiber facet to be hold stable and exactly parallel to the x,y plane.

When printing the optical device not on the fiber tip surface, but suspended on it using pillars and supporters, we developed unique technique to align the printed element to the fiber, which will detailed at 4.2.2. In that way we reached much more accurate process and devices.

Thus we are able to grow volumetric structures in the photopolymer on top of the fiber tip and can realize optical elements with it.

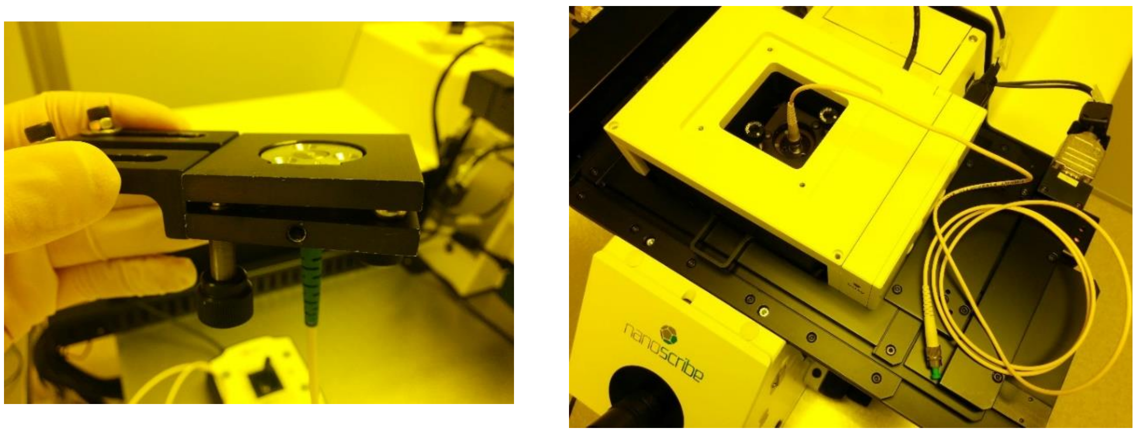

Figure 8: Technical adaptation for fiber in the system with tip-tilt correction screws, separate (left) and connected to the system (right).

3.2 Process optimization

The nanoscribe system in its original configuration is designed to create and print 3-dimensional structures, but not with optical orientation. The standard method is to design a model using common 3D designing program, and to export a standard 3D CAD file (with '.stl' extension). The nanoscribe's included software, 'nanowrite', processes that file, and outputs the '.gwl' file which is the file that hold the writing data for printing the structure. That data includes the writing parameters such as laser power, velocity, functions of the system (like finding the interface, tilt correction etc.) and most important – the path that the piezo stage required to move under the laser beam, in order to create the designed structure.

In order to optimize the printing process, and improve the printed device in terms of optical quality, many directions were studied and optimized.

3.2.1 Software development

The conventional operation principle of the 'nanowrite' software is to slice the structure to 2 dimensional horizontal layers, and design the printing process by polymerizing layer by layer bottom-up, beginning from the substrate to the end of the structure. In the software, the user can control very little of the writing process, by defining parameters like: height difference between two layers, the direction of the hatching of each layer and few more.

This method has disadvantages in creating smooth structures, and every element that has a curved surface is produced with discontinuities on the surface due to the slicing of the software. In addition, every layer of the structure is printed in one of two options – hatching the layer with straight lines, or hatching it with contours in the exact shape of the layer's margin.

Instead of using the system's software, we developed an alternative code that generates the writing file (.gwl extension) arbitrarily, in particular design for each shape and form.

Using MATLAB, we developed code that creates matrix of data. Most of the data in the matrix is the X,Y,Z points of the printing path that is designed. In between, there are printing commands and parameters. The matrix is built using functions that design many types of paths. After the matrix is completed, it is modified to .gwl file using script of macro commands in notepad++ (can be done using any word processing program) that convert the file to be in the system's format.

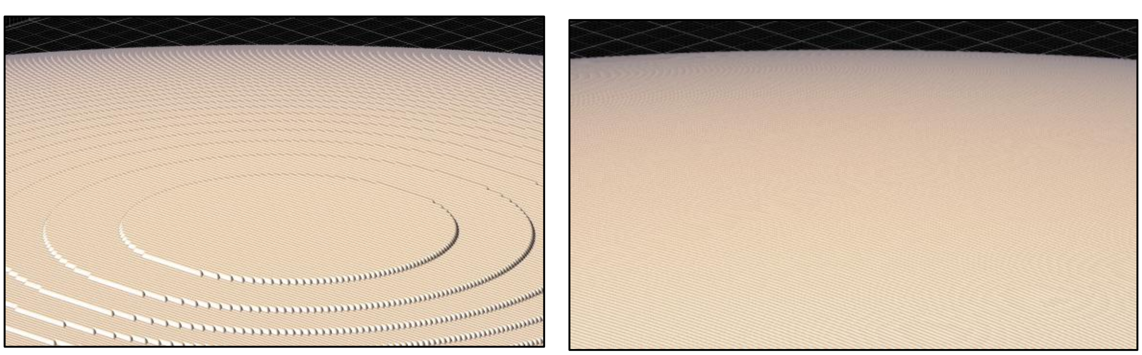

Figure 9: Example of spherical shell designed with the included software (Left) and with the developed code (Right)

An example of the difference between the nanowrite software and our intend design can be seen in figure 9. The design of a spherical lens in the nanowrite software causes the element to be printed with stair-shaped discontinuities on its surface, due to the horizontal slicing of the structure. In contrast, our design creates the element by printing it spherical shell by spherical shell, from the inner part of the shape to the outer surface, much like onion layers. Using this method, the structure is being fabricated much smoother.

3.2.2 Surface roughness optimization

One of the most important parameters in optical element is its surface roughness. In order to reach high optical quality of the fabricated elements, we optimized the writing process and reached very low surface roughness.

The fact that the writing process is performed line after line cause the surface to be rough and with noticeable pattern of the writing lines. By controlling and varying the writing parameters (laser power, velocity of the piezo stage, and pitch of written lines) we were able to reduce the roughness of the device and got very smooth surface.

Basically, there is individual dependence between each writing parameter to the quality and roughness of the printed device. The focus of the laser beam needs to stay at a specific point for only a limited time, overexposure can cause the photoresist to explode. On the other hand, the beam cannot move too fast, for accurately writing the device.

A large set of volume blocks were built while varying the writing parameters for each block and subsequently were characterized by AFM to examine the fine resolution topography. Few structures with high power and slow writing speeds and/or fine pitch experienced photoresist explosions caused by high intensity concentration at specific area for long duration (figure 10).

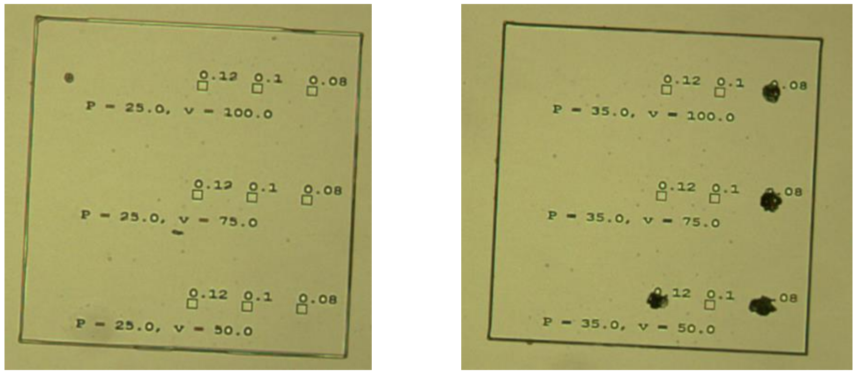

Figure 10: set of blocks for roughness optimization

We performed a Fourier Transform on the AFM scans in order to find out the spatial frequencies that exist in the surface. The writing lines create side lobes in the Fourier domain which can be seen in top of figure 11.

After optimizing the process, the best RMS roughness we reached was 4.4 nm, with velocity of 75 μm/sec and pitch of 100 nm, resulting in nearly indistinguishable writing lines on the surface. In that case the side lobes in the Fourier domain are not exist, indicating very smooth surface.

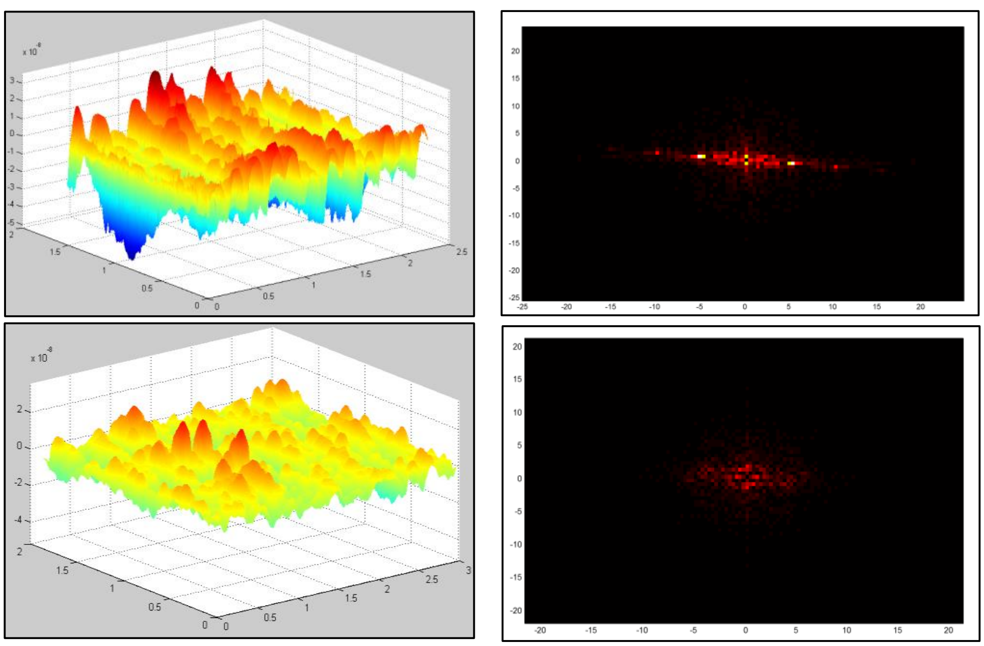

Figure 11: Top: poor roughness value. Bottom: optimized roughness. (Left is atomic force microscope topography measurement, Right is its Fourier transform. The presence of two spikes indicates the line writing topography is prominent on the left hand side).

Nevertheless, the devices we created were printed with 200 nm pitch in order to decrease the writing time. That fact didn't cause significant or noticeable reduction in the optical performance of the device.

3.2.3 Structure optimization

During the fabrication process, polymerization and development, the final shape of the structure can get deformations and inaccuracy. Many tests and iterations of printing structures were done in order to optimize the final structure after the printing process.

The structure's shape can be influenced from the path of the stage under the laser spot. In order to create a spherical lens, few path alternatives can be performed. After writing our code, we first tried to create the lens shell by shell while each spherical layer was printed with circles, one inside other. This way caused the shape to shrink asymmetrically, and produced a bump in the middle of it (figure 12). The second way we designed was using one long spiral to create each spherical shell. This had the same problems as before.

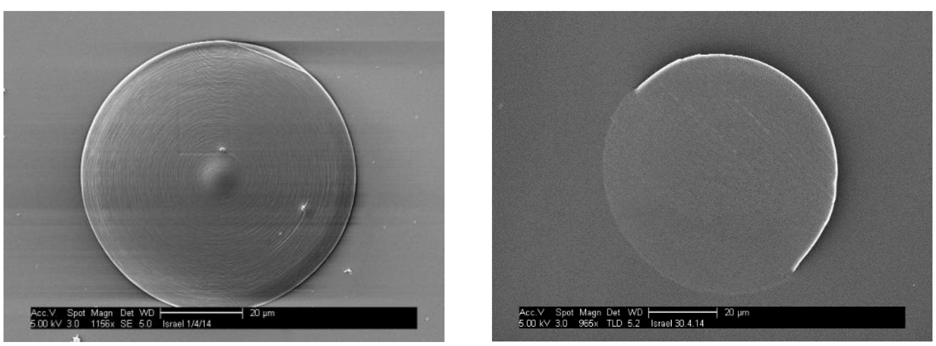

Figure 12: Structure's deformaties during fabrication process

Another problem that we encountered was disconnection of the element's base from the substrate (figure 12). The way to handle it is by changing the depth of anchoring the structure to the substrate. Each printing starts slightly below the substrate-resist interface in order to increase the adhesion of the structure.

Finally, we printed the lens by creating each spherical layer with curved lines, from one edge of the layer to the other edge of it, and in that way printing the whole lens layer by layer. The layers were printed lengthwise and crosswise, causing the structure to shrink uniformly, without a difference between the two axes.

We found that every structure or element has its own unique design and needs to be optimized in terms of shrinkage and deformities.

3.3 Printing time minimization

The writing process of 3D structure with large volume at fine pitch can take a very long time. The straightforward way to print these structures is by moving the piezo stage and polymerizing the whole volume of it, line by line and layer by layer. In order to significantly decrease the writing time, we examined writing an internal skeletal support structure for the volume's outer shell (figure 13). The writing process encapsulates the un-polymerized photoresist within the structures, in the internal chambers. After printing the outer layers of the device, we take the fiber and expose the structure to UV light which polymerizes it directly with single photon activation (conventional lithography exposure).

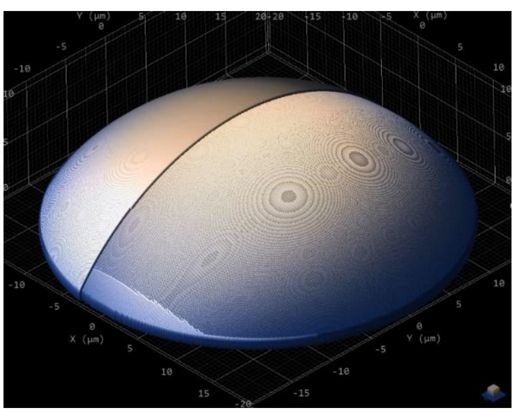

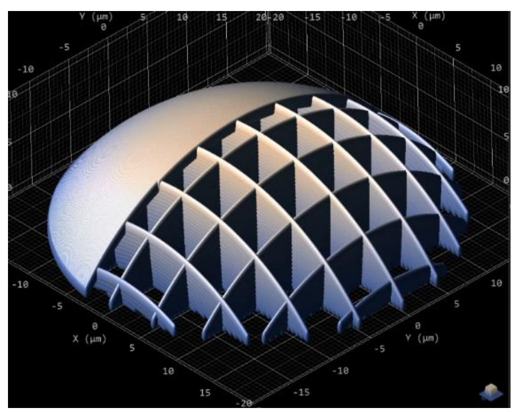

Figure 13: An example of spherical lens fabrication using the conventional method (Left) and the proposed method for decreasing process time (right). Images from DeScribe – the simulation software of nanoscribe.

First step of that procedure was checking if the outer surface can hold and trap the liquid resist inside it. For that we printed few structures only with their few outer shells. After regular development, we scratched the structures under microscope using simple toothpick, and in that way we saw the liquid resist that was trapped inside the structure's volume (figure 14).

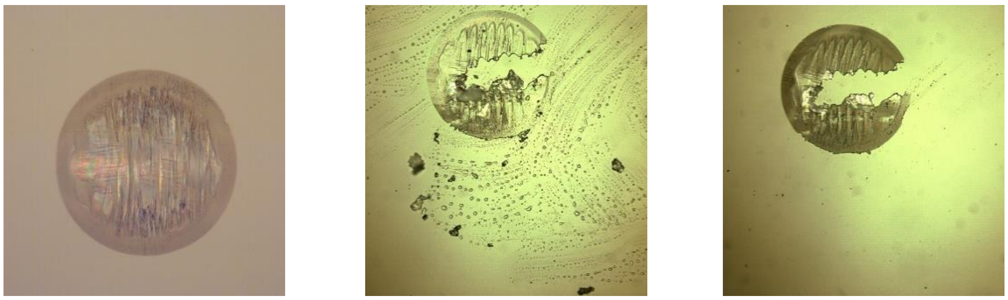

Figure 14: Test for trapping liquid inside structure. (a) the printed lens after regular development. (b) the structure after scratching it using simple toothpick. (c) the structure after cleaning it with IPA.

Next we made sure that the un-polymerized resist becomes solid using direct UV illumination, and then we illuminated the structures, getting complete polymerized device.

To demonstrate the writing speed savings, writing over the entire cubic volume of $50\mu m \times 50\mu m \times 10\mu m$ can take ~3.5 hours (at our optimized writing parameters); the same volume (skeletal structure and outer shell) can be written with the proposed method within ~30 minutes of writing time.

In the example shown here (figure 13), there is a spherical lens created with the regular technique, and with our developed one. The skeletal support is with pitch of ~5μm, rectilinear walls, and no horizontal structures.

3.4 Physical characterization methods

The characterization of the printed device was done on two levels. One is testing the outer surface roughness and the “macro” shape of the structure, and second is the optical performance characterization.

In order to check the structure's size, outer shape, and surface roughness we used few tools and methods while each has its own advantages and disadvantages.

3.4.1 Scanning Electron Microscope (SEM)

Scanning Electron Microscope (SEM) is a tool that produces an image of the tested element by scanning it with an electrons beam that interact with the sample, and produces signal which can be detected by sensors. The most common SEM mode and the one we used is detection of secondary electrons emitted by atoms that excited by the electron beam. The number of secondary electrons that can be detected depends, among other things, on the angle at which beam meets surface of specimen. By scanning the sample and collecting the secondary electrons with a spatial detector, the tool display the topography of the surface as an image.

Using the SEM, we characterize the shape of the structure, and we studied the printing and developing process, in terms of shrinkage and deformities. The SEM images show us the general form of the structure and have very good resolution to teach about the "macro" effects that carried out while printing and developing the device. However, with the SEM system it is difficult to measure properties of the structure like radius of curvature, height differences and sometimes even size.

We designed a special stage that fits and can be connected to the SEM stage, and can hold the fiber inside the vacuum cell of the system.

3.4.2 Atomic Force Microscope (AFM)

Atomic Force Microscope scans a sample surface with very high resolution. The working principle of an AFM is based on using the forces between the scanning tip and the scanned device in order to measure the surface roughness and topography. A laser beam is directed to the tips cantilever and returned to a photodiode that measure the deflection of the returned light from the center of it.

There are few operation modes of the tool, and we used the “tapping mode”, which the cantilever is driven to oscillate up and down at or near its resonance frequency by a piezoelectric element mounted in the AFM tip holder (figure 15). The interaction of forces acting on the cantilever cause the amplitude of this oscillation to decrease as the tip gets closer to the sample. The system uses a piezoelectric actuator to control the height of the cantilever above the sample. These changes of oscillations amplitude in each measured point are translated to a topography image of the sample surface.

The AFM output is the structure's surface topography in very high resolution. We used this tool mainly to characterize the roughness of the element's surface, and also to check some shape properties like radius of curvature or height differences which the SEM cannot measure well.

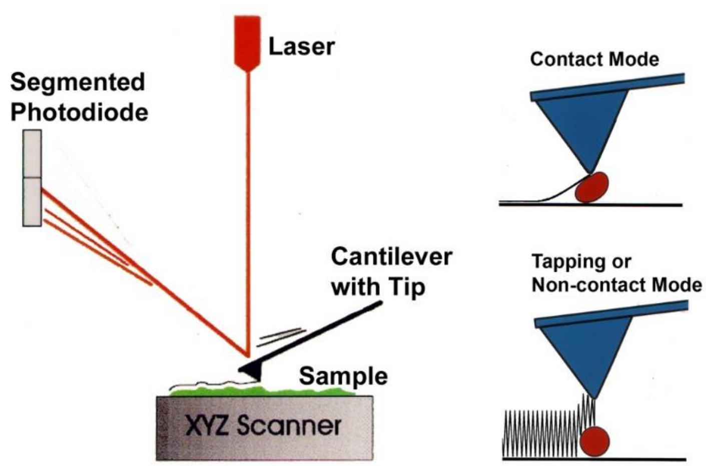

Figure 15: AFM operation principle.

The main limitation of the AFM tool is in its scanning volume, which is restricted to about 100μm×100μm in the x,y plane, and more problematic, is limited to height differences of about 5μm. that fact reduces the number of cases that we can test using that system.

3.4.3 Mechanical Profilometer

Mechanical profilometer is used to measure a surface profile cross section. That tool uses a stylus that move vertically until it gets in contact with a sample and then move laterally across the sample for a specified distance and specified contact force. A profilometer can measure small surface variations in vertical stylus displacement as a function of position. The height position of the stylus generates an analog signal which is converted into a digital signal, for generating the profile of the scanned element. The horizontal resolution is controlled by the scan speed and data signal sampling rate. In few cases, this tool helps us to measure profiles that were not possible to measure using AFM (because of the height differences).

We used the system in its weakest mode, in order to not destroy the structure during the scan.

3.5 Optical performance characterization methods

Two optical setups were built for optical activity characterization of the printed devices. One setup designed to characterize devices printed on glass substrate. In that setup there is a cleaved fiber that is held on tip tilt stage, and its tip directed to the device on the glass substrate that held on x,y,z stage, for enabling placing the device in front of the fiber tip (figure 16). Additionally, there is an IR camera with magnifying objective on x,y,z stage, that images specific plane, and captures the beam diverging from the optical element. Using this setup we could test elements on glass substrate and optimizing them before printing directly on the fiber tip.

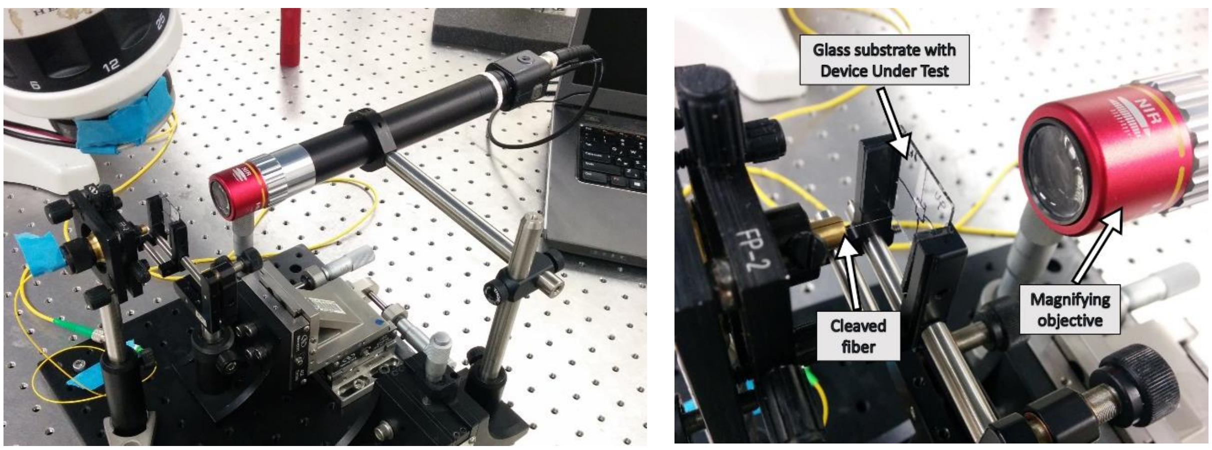

Figure 16: Optical setup for checking the elements printed on glass substrate. The setup hold cleaved fiber directed to the element on the fiber, and an IR camera with magnifying objective. Zoom in picture at right.

The other setup is very similar to the first one, but here it has fiber holder on stage with X, Y, Z, and tip tilt movements that can hold the fiber with the printed element on it, and an IR camera with magnifying objective. In order to find the fiber tip and the optical element in a comfortable way, and to focus on their planes, we installed a beam splitter and an IR illumination for projecting the fiber tip vertically, realizing a bright field microscope for the fiber and the printed device (figure 17). Before changing the setup to the bright field configuration, it was impossible to find the exact plane of the fiber tip using side illumination, and focus the camera exactly on the desired plane.

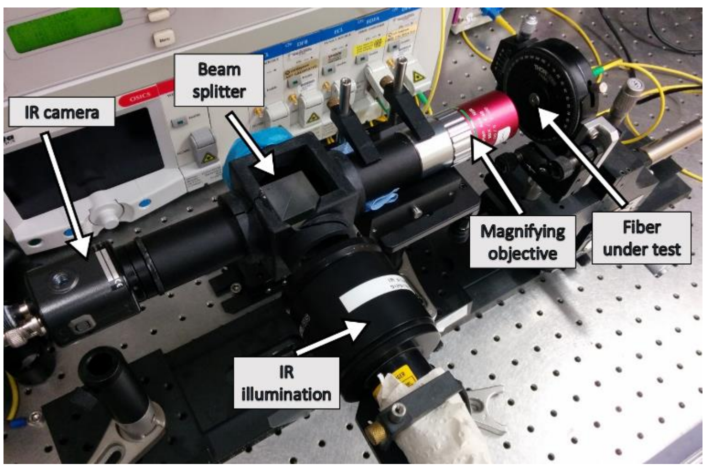

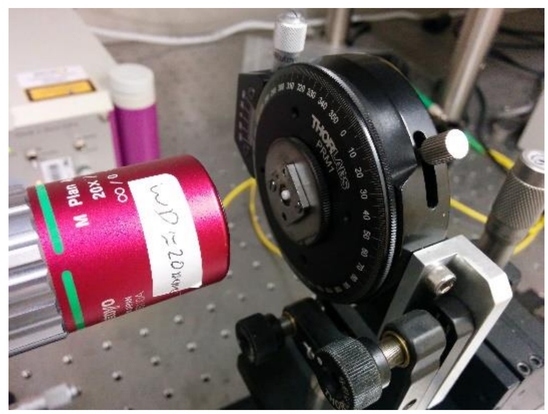

Figure 17: Optical setup for checking the elements printed on the fiber tip. The setup hold the fiber with the element on it in front of the magnifying objective. Bright field microscope with IR ilumination is implemented for easily focus on the fiber facet. Zoom in picture at right.

4 Printed devices and structures

For realizing an optical element using the nanoscribe, we created elements that interact with the light beam, and change its phase over the field distribution. The change in the phase is due to the difference in the refractive index from the polymerized structure to the air, and that can be achieved by two methods. One is the direct way in which the element is homogenous polymerized and the height profile provides difference in the optical distance that gives the required phase delay to any point on the field distribution. The second is using the Effective Medium Theory (EMT) which in that way the refractive index of the medium is effectively changed with engineering the pattern of the device, using sub-wavelength and periodic structures. That method gives the beam its required phase using the effective distribution of the refractive index.

We design and engineer the phase that the device will add to each point of the beam's field distribution, using the direct homogenous method, according to the relation between the refractive index of the material and the height profile of the element.

$$\Delta\phi_{(x,y)} = k_1 \cdot h - k_{air} \cdot h = \frac{2\pi}{\lambda_0} \cdot (\Delta n) \cdot h \rightarrow \boldsymbol{h_{(x,y)}} = \boldsymbol{\Delta\phi_{(x,y)}} \cdot \frac{\boldsymbol{\lambda_0}}{\boldsymbol{2\pi \cdot (n-1)}}$$

where $\boldsymbol{\Delta\phi_{(x,y)}}$ is the desired phase at each point (x, y) on the field, $\boldsymbol{n}$ is the material's refractive index, $\boldsymbol{\lambda_0}$ is the wavelength in vacuum, and $\boldsymbol{h_{(x,y)}}$ is the required height profile. Due to the high resolution and accuracy of the system, and the ability to create arbitrary asymmetrical profiles using the mentioned techniques we developed, we are able to realize sophisticated optical elements with high efficiency and accuracy.

4.1 Spherical lens

As a preliminary optical element, we realized a spherical lens directly on top of the fiber, using the methods mentioned before. The lens we printed was with radius of curvature of 15 μm and with base radius of 13 μm. We measured the beam that diverged from the lensed fiber and fit it to Gaussian beam parameters.

The expression of the electric field of gaussian beam, assuming linear polarized light in the x axis is:

$$E(r,z) = E_0 \hat{x} \frac{\omega_0}{\omega(z)} \exp\left(-\frac{r^2}{\omega(z)^2}\right) \exp\left(-i\left(kz + k\frac{r^2}{2R(z)} - \psi(z)\right)\right)$$

Where:

$$\omega(z) = w_0 \cdot \sqrt{1 + \left(\frac{z}{z_R}\right)^2} \;,\; z_R = \frac{\pi \omega_0^2}{\lambda} \;,\; R(z) = z\left(1 + \left(\frac{z_R}{z}\right)^2\right) \;,\; \psi(z) = \tan^{-1}\left(\frac{z}{z_R}\right)$$

We measured the width's radius of the beam $\omega(z)$ by fiting snapshots of the spot in various distances to gaussian distribution and then fiting the values of the width to curve representing the beam's divergence.

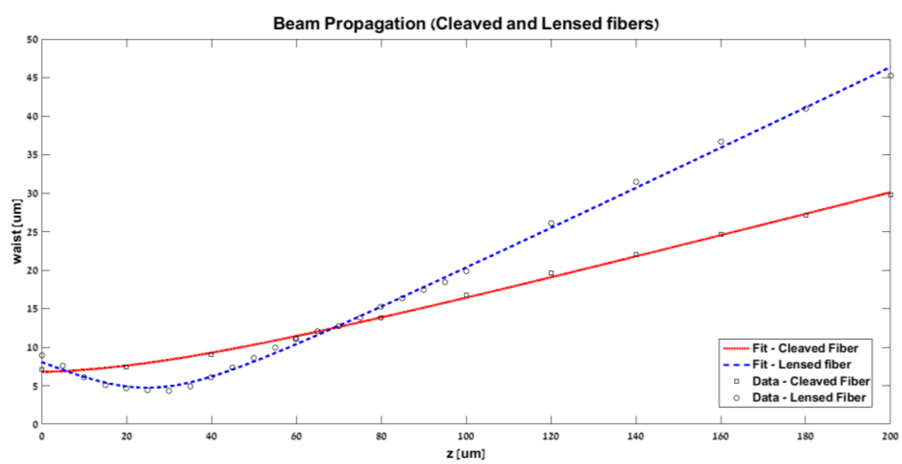

Figure 18: Measurments and fit of beam divergaence of cleaved (red) and lensed (blue) fibers.

Next, we proceeded to create more complicated devices, which are supported on construction with height of up to $150\ \mu m$.

Next element was a spherical lens which is suspended over the fiber facet at height of $100\ \mu m$ (figure 19). The beam was characterized as the previous lens, measuring the radius of the beam as function of propagation distance.

We checked the final height of the structure using regular optical microscope, by moving the focus plane from the fiber facet to the element which is on the top of the structure. By measuring the movement of the microscope head, we confirm the height of the device (with an error of $\pm 5\mu m$ because the uncertainty about the exact focus plane position due to depth of field, and the inaccuracy in the microscope z movement).

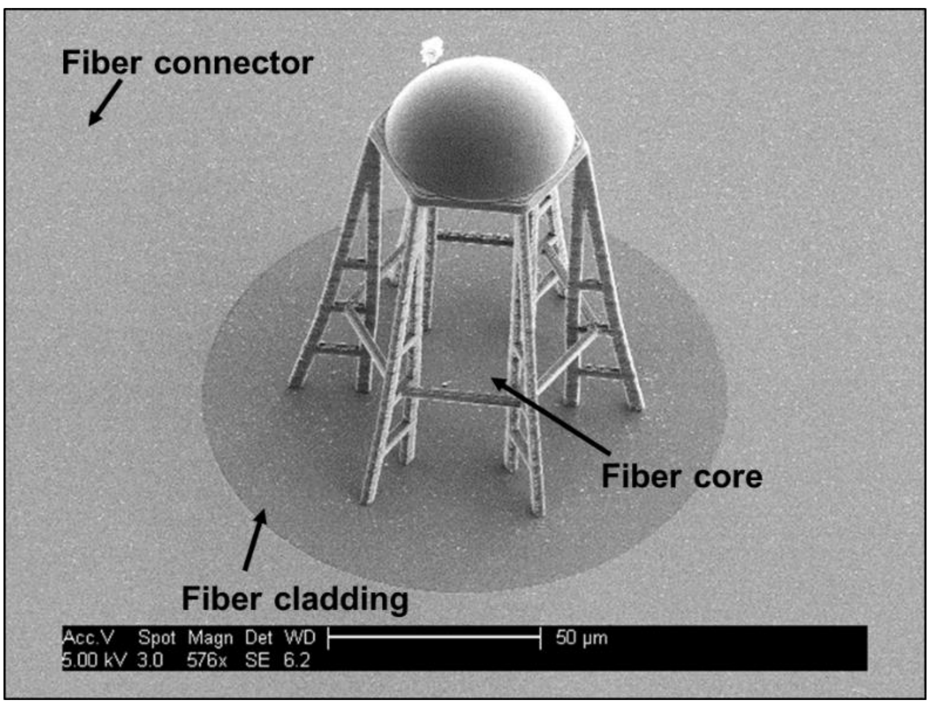

Figure 19: Suspended spherical lens printed 100 um from fiber facet.

4.2 Azimuthal phase pattern on top of collimating lens (OAM)

4.2.1 Theory - Orbital Angular Momentum of Light

A fundamental property of light is its ability to rotate when traveling in space. The common form of such rotation is the polarization rotation. At 1992 Allen et al. [5] recognized that light has another form of angular momentum originating from its helical wavefront structure, known as orbital angular momentum. Optical vortex beams have a phase singularity at the center of the optical axis and a phase factor of $exp(il\varphi)$. The orbital angular momentum of such beams can have any positive or negative integer multiple of $\hbar$[5-7].

Optical vortices have been studied extensively in various research fields. They have been used for example as rotating optical tweezers, transferring their angular momentum to microparticles and causing them to spin around the beam's axis [8]. Another reason for the special interest in these modes is the fact that they are eigen-modes of the free space and, for example, enable to implement spatial division multiplexing (SDM) in free space or any other homogenous medium.

An example of light beams carrying orbital angular momentum are Laguerre-Gaussian modes [9], described by the azimuthal index l - the number of intertwined helices, and the radial index p - the number of additional concentric rings. The LG_{lp} modes form a complete orthonormal set of solutions to the paraxial Helmholtz wave equation in cylindrical coordinates.

When $l \neq 0$, the beam has an appearance of $p+1$ annular rings, if $l = 0$, the modes have a bright central spot surrounded by p concentric rings, and when $l = 0$ and $p = 0$, the beam has a simple Gaussian profile (figure 20).

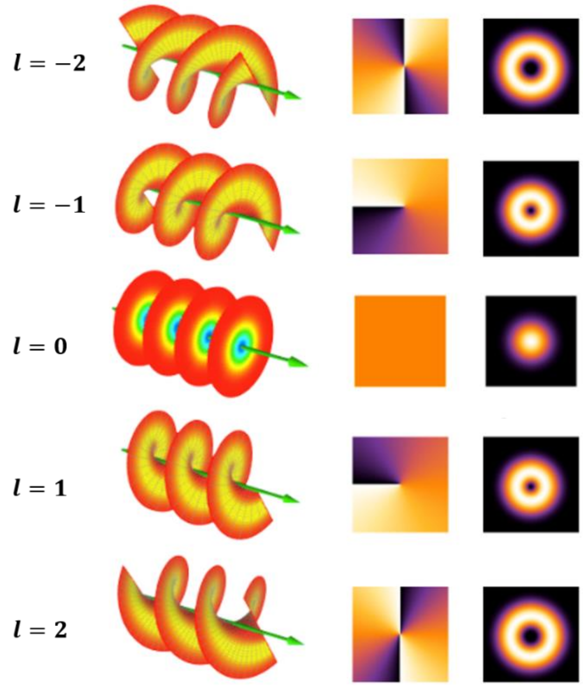

Figure 20: Beam's helical structures, phase plots and intensity pattern of a variety of LG_{lp} modes, all with p=0.

For a $p = 0$ mode, the radius corresponding to maximum amplitude can be calculated from comparing the first derivative to zero, and is given by [9,10]:

$$r(z) = \frac{w(z)}{\sqrt{2}}\sqrt{l}$$

where $w(z)$ is the beam's waist and l is the azimuthal index.

The phase pattern obviously cannot be seen in the intensity image, but with interference with a plane wave.

One of several methods that have been established to produce beams with the required azimuthal phase structure is using spiral phase plates that produce an angle dependent phase delay [11]. These are optical elements with an optical thickness that increases with the azimuthal angle. As a result, an incident Gaussian beam emerges with the helical phase front (see figure 21).

The phase delay in the discontinuity of the mask is required to be multiple of 2π and defines the step height as:

$$\Delta\phi \triangleq l \cdot 2\pi = 2\pi \cdot \frac{d}{\lambda} \cdot (\Delta n) \rightarrow \boldsymbol{d} = \frac{\boldsymbol{l \cdot \lambda}}{\boldsymbol{n-1}}$$

Where l is an integer (positive or negative) equals to the order of the mode.

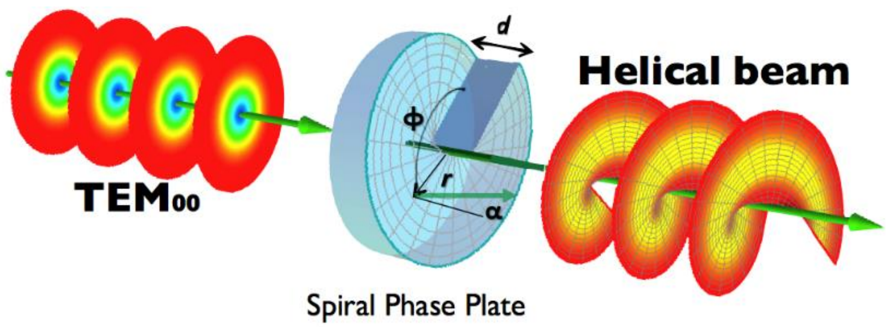

Figure 21: Spiral phase plate operation principle.

4.2.2 The printed device

The realization of the OAM mode converter was done in few steps.

First, we printed azimuthal phase masks on glass substrate, changing the printing path, making the element very smooth and accurate. We checked the accuracy of the discontinuity height and design it to give the light phase delay of multiplications of 2π at wavelength of $1550\ nm$.

We tested the elements using the optical setup for characterization in two levels. First was the intensity distribution measurement. We aligned a cleaved fiber exactly in front of each phase mask, and observed very clear ring shape at many distances (see figure 22).

Next, we moved the fiber to larger distance from the element on the glass substrate, making the light going through the element, as well as around it. In that way we caused the beam to be effectively split to two parts and interfere together in an imaging apparatus. One is the part of the beam that converted to the OAM mode, and the rest is the energy of the fundamental Gaussian mode that goes around the phase mask. Using that technique, we got the phase distribution of the OAM beam, which is a spiral pattern with number of arms respective to the mode's order (depend on the multiplication of 2π, see figure 22).

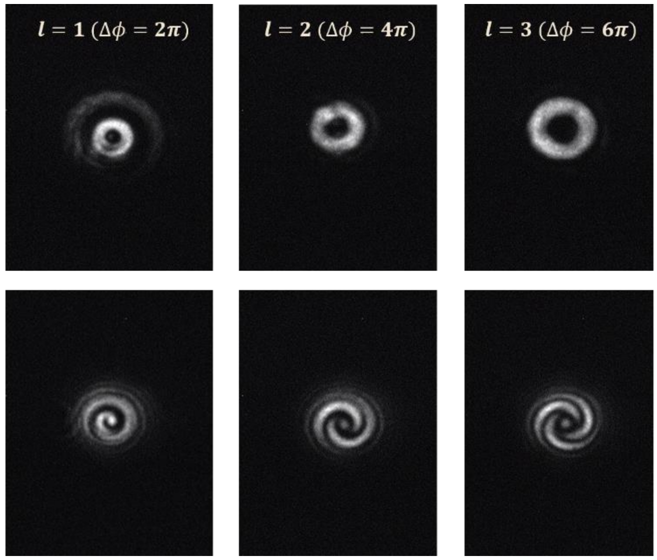

Figure 22: Intensity (top) and phase (bottom) distributions of the first three OAM modes.

After optimizing the phase plate element we proceeded to realize an OAM mode converter suspended on few fiber tips (figure 23), with and without radius of curvature, creating OAM beams which diverges in different angles.

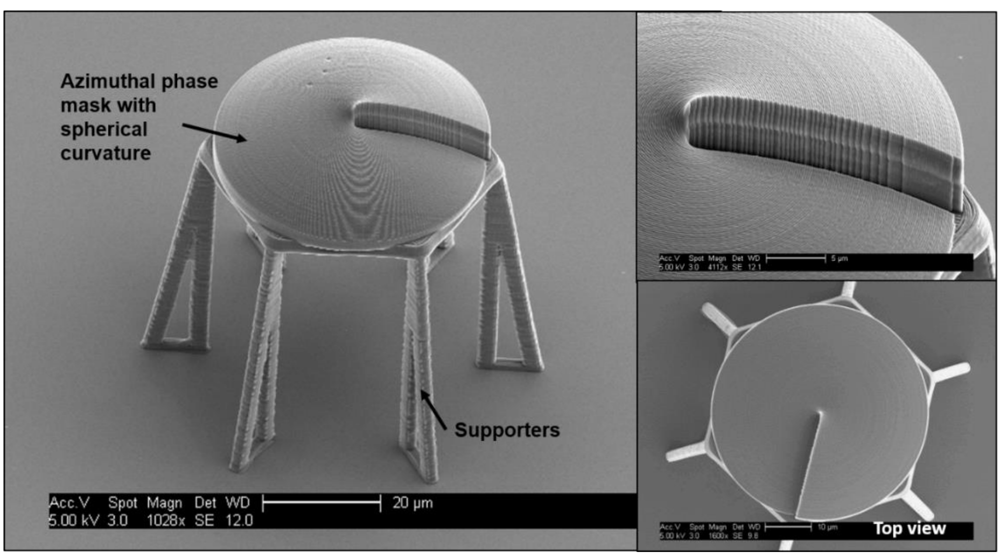

Figure 23: Suspended OAM mode converter with spherical curvature.

When printing that suspended phase plate on fiber tip, the alignment of the device relative to the optical axis of the fiber is critical in order to get the phase singularity in the middle of the beam, creating a complete ring shape.

Initially, the phase elements on the fiber didn't create complete annular intensity distribution, but shapes like 'C' or 'V' (figure 24). That inaccuracy can be caused from few reasons. One is the inaccuracy in the height of the discontinuity on the phase plate, that would not give the light phase delay of complete multiplication of 2π. Another reason can be an absorption or scattering of light in the line of the step on the plate. These reasons were rejected due to the success of generating OAM modes using that technique on glass substrate. One more reason can be shift of the device relative to the optical axis of the fiber, causing the beam to hit the phase plate not exactly on its center, creating that 'C' shape of the beam.

Figure 24: 'C' shape of beams diverges from off-axis element

Many attempts have been made in order to correct that alignment problem. Most of the efforts were to correct the tilt of the structure in relation to the fiber facet plane. We measured the tilt of the fiber by checking the interface height of the ferrule around the fiber. Then we tried to correct that tilt either by using the built in function of "tilt correction" or by directly correcting the '.gwl' file, and tilt it with the measured angles (separate angle for each axis), but with no success to create a complete ring distribution.

Another technique was to add the holder tip-tilt correction stage in order to correct the measured angle manually before beginning the printing process, as mentioned before. Using this method, we could verify that the angles were corrected by measuring the tilt of the ferrule again, but this method didn't eliminated the offset of the device.

Finally, we dealt with that problem by aligning the printing process in alternative method. After finding and centering the illuminated fiber core, we manually moved the stage to the final desired location of the planned element. In that height, we centered the cursor of the software exactly in the middle of the spot, and then moved back to the fiber tip for starting the printing process. Here we saw that the cursor is not located exactly in the center of the core, meaning that the optical axis of the fiber is not exactly perpendicular to the fiber facet (probably because of polishing the fiber tip with small angle). In that point, we corrected again the angles manually, getting the optical axis of the fiber aligned to the Z axis of the system.

In order to verify the centering of the element relative to the optical axis, we took pictures of the element while launching white light to the fiber. In figure 25 there is element that was printed with offset from the optical axis, and the optimized structure that is aligned to the beam.

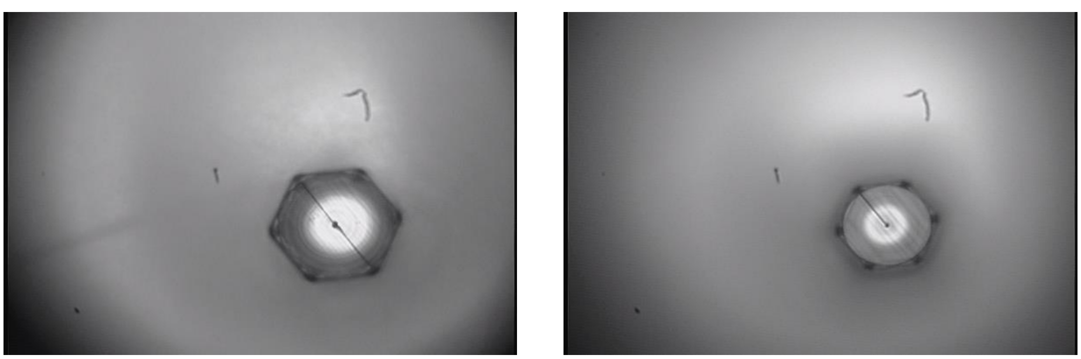

Figure 25: Suspended phase plate printed on top fiber. Illumination from the fiber shows the offset of the device form the optical axis (left) and an aligned device (right).

Using that technique we got the phase plate in the middle of the spot, creating a whole ring pattern of intensity (Figure 26).

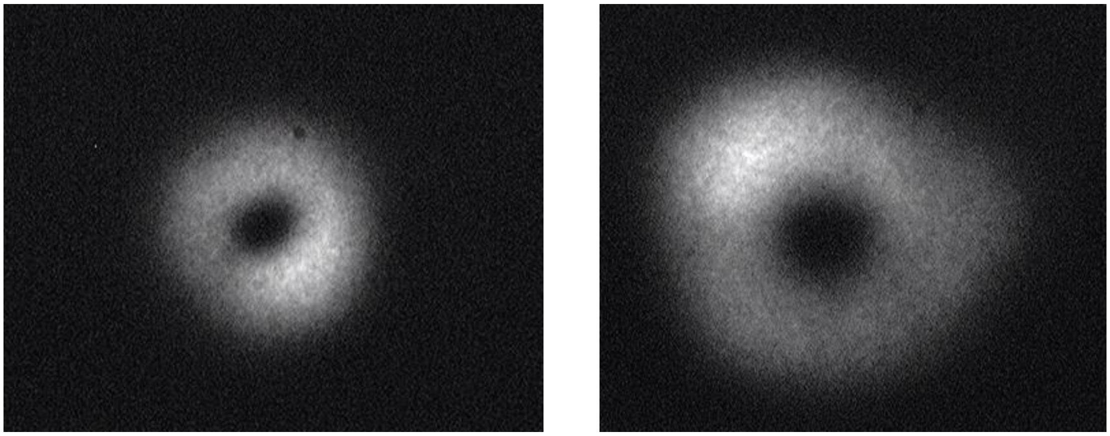

Figure 26: Annular intensity distribution diverges from OAM mode converter on top of the fiber, from two different devices

We printed OAM mode converters with various radius of curvature on it, creating OAM mode which diverges in different angles. We measured the radius of the beam diverges from flat spiral phase plate and from one with curvature as function of propagation distance, and we observed much faster divergence of the beam coming from the flat device, as expected (Figure 27).

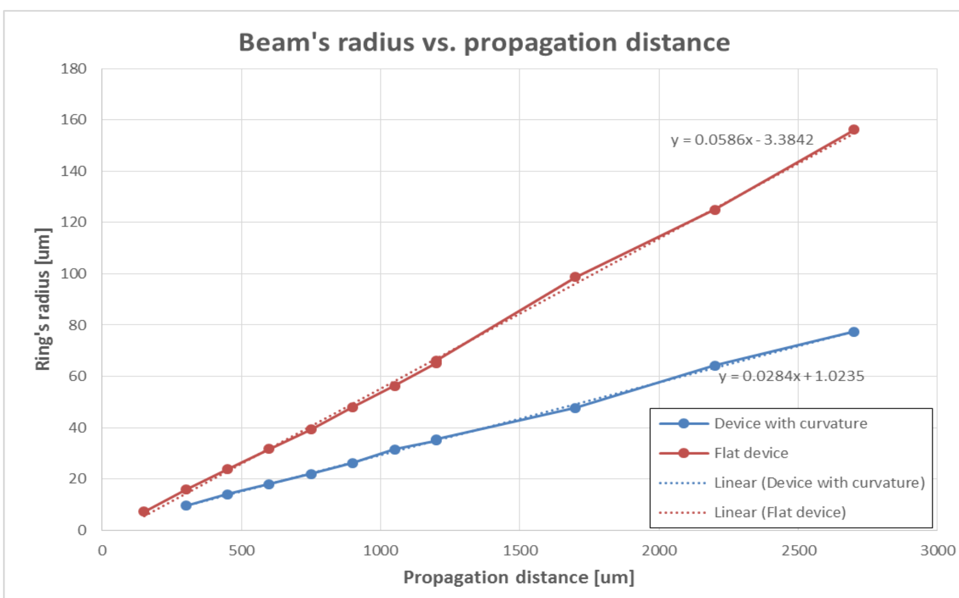

Figure 27: Measurments and linear fit of beam's radius diverges from flat spiral phase plate (red) and from one with curvature (blue).

5 Conclusions and future work

The purpose of this research was to develop a unique process of realization of real 3D micro optical elements directly on top of optical fiber. For this goal we used the commercial 3D laser lithography system of Nanoscribe.

Many adaptations and modifications have been done in order to utilize the system to realize optical elements. We were able to design and create asymmetrical arbitrary structures that cannot be realized with standard lithography techniques or other fabrication methods.

The two main issues that we dealt with were the optical quality of the device, especially in terms of surface roughness, and the alignment of the device to the optical axis of the fiber.

After many efforts and iterations, and by developing methods that are detailed before, we developed a consistent repeatable process which enable us to create arbitrary optical elements which are either attached to the fiber facet, or suspended above it by printed supporters, with high accuracy and optical quality.

Many research directions can be taken using the technology of nano-printing on top of fiber tip. In that work we demonstrated realization of linked as well as suspended bulk micro-optical elements, which serves as phase plates to the beam diverging from the fiber. Additional possibility is to scale down and to realize metasurfaces and metamaterials by printing arrays of nanostructures, using the effective medium theory.

Initial attempts were made in order to realize such structures. We started with optimizing the final shape of such nano-pillars. Initially, the structures which were designed to be with square shape, were printed in strange shapes (figure 28). After optimization and different design of the printing path, we got very good shape of squared pillars printed next to each other.

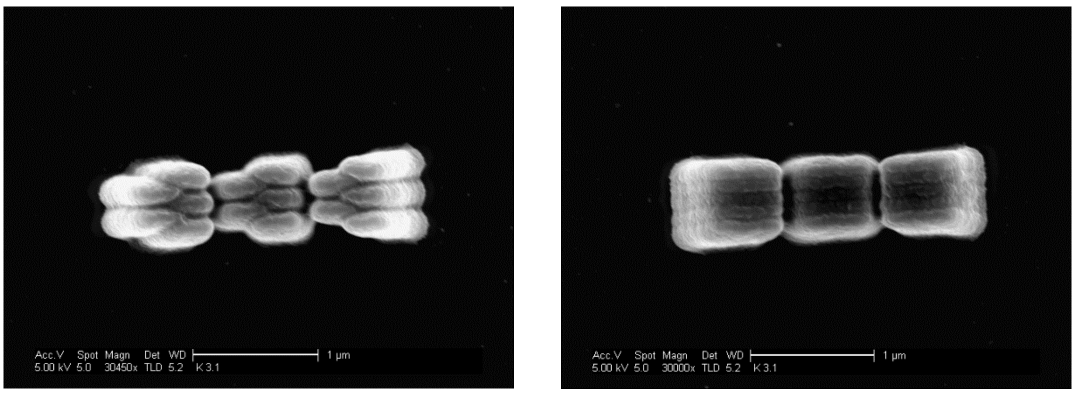

Figure 28: Top view of three pillars at the initial shape (left) and at the optimized square shape (right), with height of ~2um, and width of 0.7um.

Another effect that we encountered was sticking of the pillars after development to many groups (figure 29). An optional solution is to create thin layers or supporters every certain height to separate the pillars but with no effect on the optical performance.

This field is one example of scaling down to the nano regime using the nanoscribe system, in order to realize advanced optical devices.

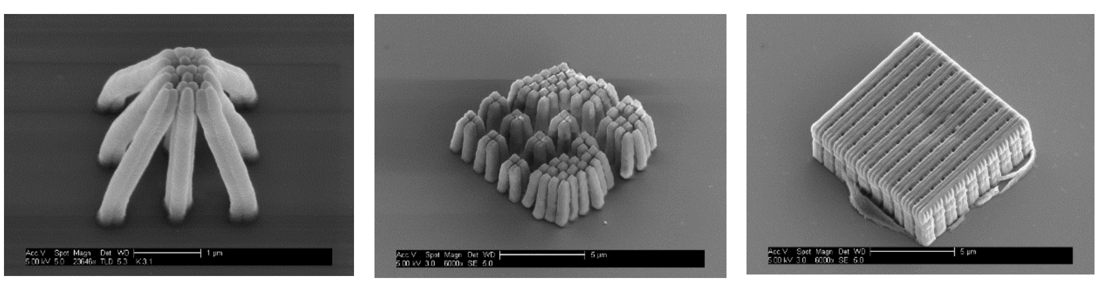

Figure 29: group of 3X3 (left) and 10X10 (middle) linked pillars and 10X10 pillars with supported thin layer (right).
Width of 0.3um (left) and 0.7um (middle and right), and height of ~5um.

6 References

1. B. Park, J. Provine, I. W. Jung, R. T. Howe, and O. Solgaard, “Photonic Crystal Fiber Tip Sensor for High-Temperature Measurement,” IEEE Sensors Journal 11, pp. 2643-2648, 2011.

2. G. Kostovski, P. R. Stoddart, and A. Mitchell, “The Optical Fiber Tip: An Inherently Light-Coupled Microscopic Platform for Micro- and Nanotechnologies,” Adv. Mater. 26, pp. 3798–3820, 2014.

3. F. Schiappelli, “Efficient fiber-to-waveguide coupling by a lens on the end of the optical fiber fabricated by focused ion beam milling,” Microelectron. Eng. 73–74, 397–404 (2004).

4. S. Cabrini, C. Liberale, D. Cojoc, A. Carpentiero, M. Prasciolu, S. Mora, V. Degiorgio, F. De Angelis, and E. Di Fabrizio, “Axicon lens on optical fiber forming optical tweezers, made by focused ion beam milling,” Microelectron. Eng. 83, 804– 807 (2006).

5. L. Allen, M. Beijersbergen, R. Spreeuw, and J. Woerdman, “Orbital angular momentum of light and the transformation of Laguerre–Gaussian laser modes,” Physical Review A, vol. 45, pp. 8185–8189, 1992.

6. A. T. O’Neil, I. MacVicar, L. Allen, and M. J. Padgett, “Intrinsic and Extrinsic Nature of the Orbital Angular Momentum of a Light Beam,” Physical Review Letters, vol. 88, p. 053601, 2002.

7. M. S. Soskin, V. N. Gorshkov, M. Vasnetsov, J. T. Malos, and N. R. Heckenberg, “Topological charge and angular momentum of light beams carrying optical vortices,” Physical Review A, vol. 56, pp. 4064–4075, 1997.

8. H. He, M. E. J. Friese, N. R. Heckenberg, and H. Rubinsztein-Dunlop, “Direct Observation of Transfer of Angular Momentum to Absorptive Particles from a Laser Beam with a Phase Singularity,” Physical Review Letters, vol. 75, pp. 826–829, 1995.
9. L. Allen, M. J. Padgett, and M. Babiker, “The Orbital Angular Momentum of Light,” Progress in Optics, vol. 39, p. 291, 1999.
10. M. J. Padgett and L. Allen, “The Poynting vector in Laguerre–Gaussian laser modes,” Optics Communications, vol. 121, pp. 36–40, 1995.
11. M. W. Beijersbergen, R. Coerwinkle, M. Kristensen, and J. P. Woerdman, “Helicalwavefront laser beams produced with a spiral phaseplate,” Optics Communications, vol. 112, pp. 321–327, 1994.